A Kinetic Model for Olefin Polymerization in High-Pressure Autoclave Reactors

Wai-Man Chan
Technology Center, Poliolefinas S.A., Av. Presidente Costa e Silva, 400, Santo André, São Paulo, Brazil 09270

Paul E. Gloor and Archie E. Hamielec
McMaster Institute for Polymer Production Technology, Dept. of Chemical Engineering, McMaster University, Hamilton, Ont., Canada L8S 4L7

Free radical copolymerization in high-pressure autoclave reactors is studied by developing a mathematical model. Kinetic mechanisms to describe the polymerization rate, molecular weight averages, branching frequencies, as well as copolymer composition are presented. Two phase kinetics due to polymer-monomer solubilities in the reaction mixture are taken into account. Gel formation from cross-linking reactions is also analyzed. A mixing model is developed to represent the stirring effect inside the reactor. The mathematical model is implemented as a computer program to simulate commercial autoclave reactors. PID control equations are used to maintain operation at the unstable steady state. A sensitivity study is performed on the mixing model parameters and on some of the kinetic parameters and the model is compared to rate data from commercial reactors.

Introduction

Low density polyethylene and copolymers are thermoplastics which are used in a large variety of applications. Generally they are produced in either autoclave type or tubular reactors. This work develops a mathematical model for the production of low density polyethylene and copolymers in high-pressure autoclave type reactors. The vessel type reactors typically operate at lower temperatures and pressures than do tubular reactors, and they behave more like a continuous stirred tank reactor (CSTR). The autoclave reactors may have a length to diameter ratio of between four and 20. Mixing is provided by a shaft running down the center of the vessel with several (up to 40 or so) impeller blades of different types. Heat transfer through the walls is limited, so that the reactor is essentially adiabatic and cooling is provided by the inflow of cold monomer. The inflow of initiator at several points down the reactor vessel provides control of the temperature which may vary down the length of the reactor. A schematic of a typical autoclave type reactor is shown in Figure 1.

The mechanism and kinetics of this free radical copolymerization is outlined by Zabisky et al. (1992). However, there are several complications which make the modeling of autoclave type reactors highly challenging, namely: nonideal mixing, the presence of unstable steady states, the existence of reactions in two phases and the possibility of gel formation due to cross-linking reactions. In order to develop a comprehensive model capable of predicting the actual plant operating conditions as well as the polymer properties, one must address all of these items without making the model too complex to be readily solved. Attempts have been made to model this type of reactor (Georgakis and Marini, 1982; Marini and Georgakis, 1984), but we are endeavoring to produce a more comprehensive model to describe not only the rates of reaction, but also the molecular properties of the material formed. Our objective is to create a mathematical structure to account for the rate of polymerization and to describe the molecular weights, compositions, branching frequencies and gel content of the polymer formed. This model includes thermodynamic and kinetic considerations for a heterogeneous reaction mixture and includes a mixing model to account for the flow pattern within the reactor. The model is put together to create a dynamic simulation of commercial autoclave reactors including multiple feed points and temperature controllers.

In this article we shall outline the important features of this model and present some simulation results in the form of sensitivity studies and comparisons with an industrial reactor.

Correspondence concerning this article should be addressed to W.-M. Chan.

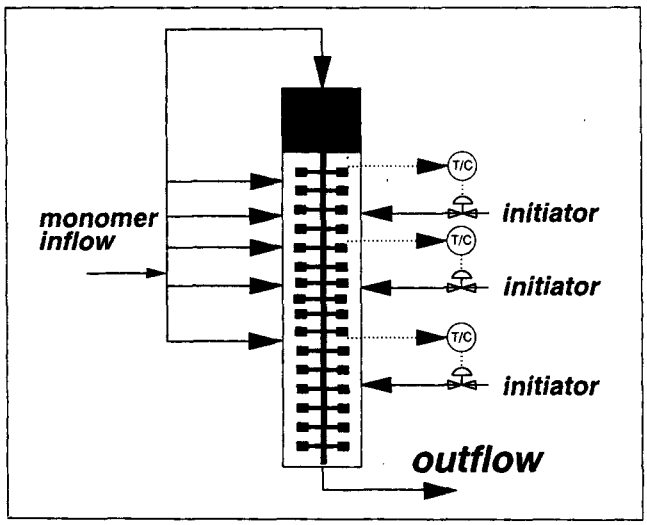

Figure 1. Typical autoclave reactor.

T/C denotes a temperature controller that manipulates the initiator flow.

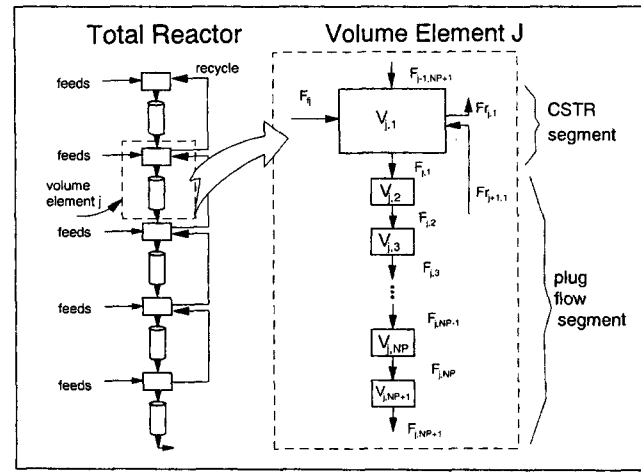

Figure 2. Proposed mixing model for total reactor and a blowup for a specific volume element *j* showing how the plug-flow segment is approximated by several small CSTRs.

The Mixing Model

The mixing pattern in an autoclave type reactor tends to be of a recirculating nature. The effect of mixing on reactor performance is very important, especially since an imperfectly mixed vessel requires more initiator per unit of polymer produced than does a more perfectly mixed vessel under the same conditions (Georgakis and Marini, 1982). The initiator tends to decompose near the feed points, and not in the bulk of the reactor, thus not promoting as much polymerization as if the initiator was uniformly distributed throughout the reaction mixture. The temperature gradients down the reactor also suggest imperfect mixing.

Donati et al. (1981) studied a cold mockup of an industrial scale reactor, a CSTR with a single impeller. They found the flow in this compartment tended to be downward near the wall, with backflow in the center. They modeled this flow pattern as two annuli divided into several CSTR's with axial flow and radial mixing between the two annuli. The regions near the impeller and the bottom of the tank were modeled as CSTR's with no radial gradients. Georgakis and Marini (1982) modeled this same reactor as three CSTR's in series with recycle to each one. They used two small volumes near the initiator feed points and then a larger volume element for most of the reaction. These models which appear to be adequate for a single compartment, at least with respect to initiator consumption, are based upon measurements of the velocities in the actual reactor and therefore should be quite realistic. However these models were proposed only for a single compartment between the stirrer blade and the bottom. Our model must account for the entire vessel.

Consider the autoclave reactor represented by N_v volume elements, each of them consisting of a CSTR segment followed by a plug-flow segment to account for steep temperature gradients from one volume element to the next. In the plug-flow segment, to avoid solving partial differential equations, we have approximated the whole section by N_p CSTR's in series. To account for recirculation we allow recycle from the CSTR segment of each element to the CSTR segment of the element above. Figure 2 shows the multiple reaction volume scheme.

We can set the volume of each element, V_j. Moreover, for each volume element we define the volume fraction of the CSTR segment to the total volume of element j as.

$$\theta_j = \frac{V_{j,1}}{V_j} \tag{1}$$

and thus θ_j is a parameter to be estimated for each volume element j. The larger θ_j the more the mixing in the element approaches ideal CSTR. The volume of each small CSTR in the plug-flow segment is given by

$$V_{j,L} = \frac{V_j(1-\theta_j)}{N_p} \qquad L = 2, 3, \ldots, N_p + 1 \tag{2}$$

The recycle is specified by a recycle ratio, q_j, defined as the volumetric flow rate in the recycle stream divided by the sum of volumetric feed rates to all elements. Thus the parameters which define the mixing model are: the number of volume elements (N_v), the volume fraction of each element that is the CSTR segment (θ_j), the number of smaller CSTR's in the plug-flow segment (N_p), and the recycle rate for each segment, except top element (q_j). Reasonable estimates of these parameters can be obtained from knowledge of the reaction temperature profile, initiator flow rates and stirrer geometry.

The Unstable Steady State

It has been found (Georgakis and Marini, 1982; Marini and Georgakis, 1984 and this article) that when using a steady-state model, one cannot solve both the mass and energy balances for reasonable operating conditions. Considering a single adiabatic CSTR, the monomer conversion given by the steady-state energy and by the mass balance can be plotted against reaction temperature (Figure 3). There is a steady state near the region where the industrial reactor normally operates, de-

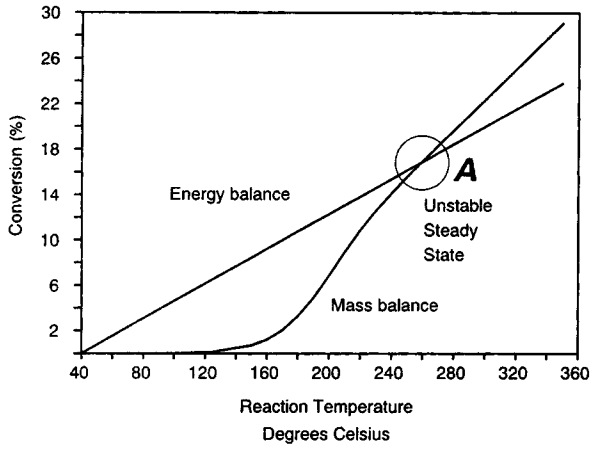

Figure 3. Steady-state operating lines for a vessel reactor based on mass balance and energy balance.

A single well mixed volume, feed temperature 40°C, ethylene homopolymerization.

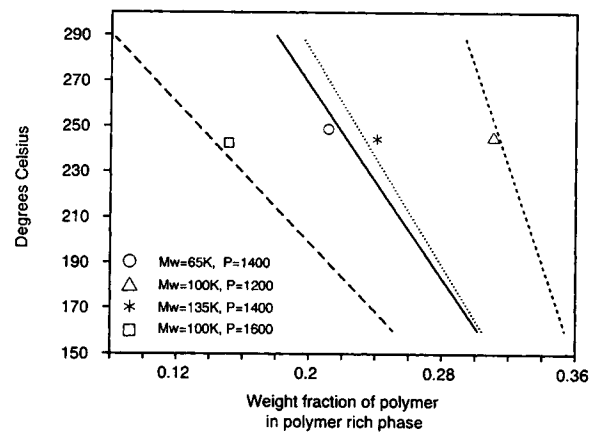

Figure 4. Phase diagram for ethylene-polyethylene from simplified correlation (Eq. 3).

noted by point A. Here both the mass and the energy balance equations are satisfied. If we attempt to operate at a point on the mass balance line to the right of point A then the heat generated by the reaction will cause the temperature to rise. On the other hand, if we start at a point on the lefthand side of A, the system will cool down until no polymerization occurs. Thus point A is an unstable steady state. One can use a dynamic simulation and include temperature controller equations to maintain the operating point at the desired steady state.

A Thermodynamic Correlation for Polymer-Monomer Phase Compositions

Under certain conditions, the polymer may precipitate out from the monomer, forming monomer and polymer rich phases. The polymerization then occurs as a heterogeneous reaction. Reactions with dead polymer, like branching and ultimately gel formation reactions, are accentuated in the polymer rich phase. It has been reported that the polymer produced under heterogeneous conditions differs significantly from the polymer manufactured under homogeneous conditions, the former providing a better balance of mechanical and optical properties (Bogdanovic and Srdanovic, 1986). It is of vital importance to quantify the polymer-monomer compositions in each phase during the polymerization. The boundary between homogeneous and heterogeneous reaction conditions is a function of pressure, temperature, and polymer structure.

In order to quantify the monomer and polymer compositions in each phase of the reaction mixture, a joint project was undertaken by Poliolefinas and the group of Prausnitz at the University of California, Berkeley, to model the phase equilibrium problem in polymeric systems using the continuous thermodynamics approach and a cubic equation of state (Sako et al., 1989). This resulted in the creation of a software package entitled PFLASH (1988). PFLASH calculates the weight fraction of polymer in each phase as a function of temperature, pressure and molecular weight. For ethyene-polyethylene, this model predicts an insignificant amount of polymer dissolved in the monomer rich phase under the normal range of operating conditions, so we need only concern ourselves with the monomer concentration in the polymer rich phase.

Due to the relatively large computation time required to run the complex thermodynamic model (PFLASH), a much simpler correlation was developed by fitting the output generated by PFLASH. Simulations were performed using PFLASH following an orthogonal factorial design and multiple linear regression was used to calculate the eight coefficients (Box et al., 1978). All coefficients were significant at the 95% confidence level.

$$W_t = 0.24548 - 0.05777X_1 - 0.078337X_2 + 0.0048718X_3 - 0.027386X_1X_2 + 0.0032556X_1X_3 + 0.003281X_2X_3 + 0.0029964X_1X_2X_3 \quad (3)$$

where W_t is the weight fraction of polymer in the polymer rich phase, and X_1, X_2, X_3 are all normalized variables defined as:

$$X_1 = \frac{T(K) - 498.2}{65} \qquad X_2 = \frac{P(Kgf/cm^2) - 1{,}400}{200}$$

$$X_3 = \frac{\overline{M}_w - 100{,}000}{35{,}000}$$

This correlation is only valid when all the normalized variables fall within the range of $[-1, +1]$. Due to our lack of data for the ethylene-vinyl acetate-polymer phase relationships under these conditions, this correlation is only strictly valid for ethylene and polyethylene. The presence of vinyl acetate has not been taken into account. Figure 4 shows the sensitivity of W_t to temperature, pressure and weight average molecular weight, and Figure 5 shows the fit for the simplified correlation to the PFLASH calculations.

Gel Formation

Gel is an insoluble polymer network that can be formed under certain reaction conditions, and greatly affects final product properties. By definition, the onset of gelation occurs when the weight average molecular weight ($\overline{M}_w$) goes to infinity. Gel formation is caused by the branching reactions between

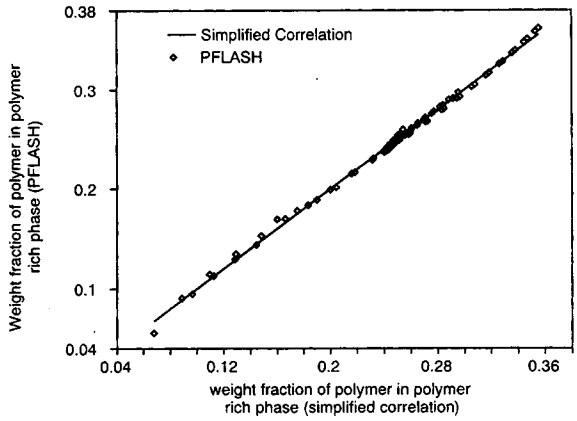

Figure 5. PFLASH predictions vs. predictions from simplified correlation (Eq. 3).

radicals and dead polymer including transfer to polymer followed by termination by combination and reactions with terminal double bonds in polymer chains. When the polymer concentration in the polymer rich phase becomes very high, branching reactions and eventual gelation are accentuated. The gel, once formed, acts like a sponge rapidly consuming sol polymer molecules and radicals. One can identify the following reactions as responsible for the gel growth: addition of monomer to gel radicals by propagation, termination by combination of sol radicals with gel radicals, reaction of sol radicals with terminal double bonds in gel, and reaction of gel radicals with terminal double bonds in sol.

In our system, the double bonds on polymer chain ends are produced by β-scission, transfer to monomer, and termination by disproportionation type reactions. To account for the reactions with double bonds, one must keep track of all polymer chains with and without double bonds, thus significantly complicating the molecular weight calculations. However, our simulation shows that adequate branching frequencies can be obtained by simply including transfer to polymer reactions. Therefore we shall ignore reactions with terminal double bonds to reduce the complexity of the problem and accept that our model may be deficient in this regard.

Model Development

Polymerization reaction mechanisms considered

In this work, the following elementary reactions (Table 1) are included from the set presented by Zabisky et al. (1992). Initiation is by thermal decomposition of an organic peroxide initiator. The modifier acts as a chain transfer agent, but may also be incorporated into the chain in small amounts to contribute to the short chain branching. The first subscript in the rate constants refers to the type of radical center, and the second describes the monomer type. R' represents a backbone radical center, $R^=$, $P^=$ denotes a radical or a polymer with a terminal double bond.

Pseudo kinetic rate constants

One can simplify the mathematical equations for a copolymerization by using pseudo kinetic rate constants as outlined by Hamielec et al. (1987) and Zabisky et al. (1992). Instead of writing down all the reactions between all monomer or radical types, we can formulate the equations in terms of the total monomer or radical concentrations. Our mass and energy balances then appear as homopolymer equations but will be valid for copolymerizations.

Overall balances

Given the mixing model, one can construct the mathematical model by writing the mass and energy balances for a single volume segment (recalling that a volume element is composed of 1 main CSTR segment and 1 plus flow section approximated by a variable number of CSTR's referred to as plus-flow segments). The resulting set of differential equations, for all volume segments, must usually be solved simultaneously because of the recycle. The mass balance for a species in a volume segment will, in general, have the form:

accumulation in volume segment
= outflow from previous segment
+ feed to segment
+ recycle from next element
− outflow to next segment
− recycle to previous element
+ net generation by reaction (4)

For the plug-flow segments there will not be any feed, or recycles. We must perform population balances on monomer and comonomer, moles of each monomer bound as polymer, initiators, radicals and modifier. The stationary state hypothesis is used for all radical species. The details of the mass balance equations are given in the appendix.

Two phase kinetics

We need to determine the rate of reactions. Since the concentrations of each species may be different in each phase we must consider the contribution of reaction in each phase to the overall rate of reaction. The following assumptions are adopted for the two phase kinetics.

- Thermodynamic equilibrium. The amount of polymer in the monomer rich phase is negligible. The monomer-polymer compositions in the polymer rich phase are determined by the simplified correlation (Eq. 3).
- In calculating the volume fraction of each phase, the volumes are considered to be additive.
- The ratio of vinyl acetate to ethylene monomer concentrations will be identical in both the monomer and polymer rich phases.
- The kinetic rate constant values are the same in both phases.
- Initiator, modifier and radical concentrations in each phase can be described by partition coefficients. The radical partition coefficient value is equal to the square root of the initiator partition coefficient.

The details of the equations for the volume fractions of each phase, the mass balances for each species and the rates of reaction in each phase are given in the appendix.

Table 1. The Kinetic Scheme

I	$\xrightarrow{k_d}$	$2 \cdot R$	Initiation
$R_j(r) + M_i$	$\xrightarrow{kp_{ji}}$	$R_i(r+1)$	Propagation
$R_j(r) + M_i$	$\xrightarrow{kfm_{ji}}$	$R_i^{=}(1) + P(r)$	Transfer to monomer
$R_j(r) + TS$	$\xrightarrow{kfts_j}$	$TS^{*} + P(r)$	Transfer to modifier
$R_j(r) + TS$	$\xrightarrow{kpts_j}$	$R(r+1)_{\text{short branched}}$	Modifier incorporated in the chain
$R_j(r) + P_i(s)$	$\xrightarrow{kfp_{ji}}$	$R_i'(s) + P(r)$	Transfer to polymer (long chain branching)
$R_j(r)$	$\xrightarrow{kb_{ji}}$	$R_i'(r)$	Backbiting (short chain branching)
$R_j(r)$	$\xrightarrow{k_\beta}$	$P^{=}(r-1) + R_j(1)$	β-Scission of terminal radicals
$R_i(r) + R_j(s)$	$\xrightarrow{ktc_{ij}}$	$P(r+s)$	Termination by combination
$R_i(r) + R_j(s)$	$\xrightarrow{ktd_{ij}}$	$P^{=}(r) + P(s)$	Termination by disproportionation

Molecular weight equations

The molecular weight equations, using the method of moments, are as outlined by Hamielec et al. (1987), and Tobita and Hamielec (1989a), with some modifications for polymerization in two phases. The leading moments for radical and polymer chain length distribution for each phase are explained in the appendix. Since at the gel point, the weight average molecular weight goes to infinity we need to carry out the molecular weight moment analysis under two distinct domains, namely pregel and postgel regions. In the postgel region, only the molecular weight averages of the sol are calculated. After the gel point, the polymer moment equations are not closed. The i^{th} moment depends on the $(i+1)^{th}$. For this reason, we must use a closure technique in order to calculate the higher moments as a function of the lower ones. The transfer to polymer rate is a function of the higher moments. In the pregel region the transfer to polymer reaction, assuming the stationary state hypothesis for radicals, causes no net change in the number of radicals. Thus for the second moment, these terms cancel out and the moment equations are closed. However, in the postgel region, this reaction causes radical centers to move between the sol and the gel phases and thus we can no longer cancel out these terms, and the moment equations are not closed. We have selected the method of Hulburt and Katz (1964) although the validity of this method should be checked by comparison with actual data (Zabisky et al., 1992). If molecular weight data are available, the closure equation then should be obtained by fitting a correlation to this data in order to get more accurate results. We should note that obtaining accurate molecular weight averages (M_n, M_w, M_z) is not a trivial task for branched polymers and copolymers.

$$[Q_3] = \frac{[Q_2]}{[Q_1][Q_0]} \left(2[Q_2][Q_0] - [Q_1]^2\right) \tag{5}$$

Balances are made on short and long chain branches to determine the branching frequencies. Since the concentration of polymer in the monomer rich phase is negligible, reactions with dead polymer are only considered in the polymer rich phase.

The mass of gel is calculated and is assumed to reside only in the polymer rich phase. At the gel point, the mass of gel must be given some positive, nonzero value, however, it is unclear just what this initial value should be. Tobita and Hamielec (1989a) defined a possible initial condition based upon conversion and cross-link density, but the condition is still somewhat arbitrary. Moreover, the gel growth equation does not appear to be very sensitive to the value chosen, therefore for simplicity, we have arbitrarily set the initial gel fraction to a small value (about 10^{-2} or 10^{-3}). The gel point is defined as the point where the weight average molecular weight becomes infinite. For practical purposes, we cannot calculate infinite molecular weights, so we must arbitrarily state a maximum molecular weight that is effectively infinite. It is fortunate that at the gel point, the weight average molecular weight grows very rapidly with increasing cross-link density, so that the practical gel point is not sensitive to the maximum molecular weight value chosen. Alternatively, one could specify a large polydispersity (M_w/M_n) which would appear as a scaled maximum molecular weight.

Details of all these equations are given in the appendix.

The energy balances

Calculation of the temperature profile along the reactor length and the initiator flow rates requires an energy balance on the reactor contents that accounts for the inflows, outflows, recycles and the reactions. The reactor is assumed to be adiabatic and the only cooling is supplied by cold monomer feed. Heat generation is from the propagation reaction only. The energy balance equation is given in the appendix.

Temperature controller equations

The autoclave reactor temperature is controlled by manipulating the initiator feed. The controller is of a continuous proportional-integral-derivative type.

$$F_I = F_{I_{ss}} + K_p(T_{\text{set}} - T) + \frac{K_p}{\tau_I}\int_0^t (T_{\text{set}} - T)dt + K_p\tau_D \frac{d(T_{\text{set}} - T)}{dt} \tag{6}$$

F_I is the initiator flow rate. The subscript ss denotes steady-

state (or initial value) of the initiator flow. T_{set} is the set point temperature, T is the measured temperature and the parameters K_p, τ_I and τ_D are the proportional gain, integral and derivative time constants respectively. Temperature is controlled in the CSTR segments only and the initiator flow does not necessarily enter the element that is being controlled. For example, the temperature at the bottom of the reactor may be controlled by manipulating an initiator flow entering at the mid-point of the reactor length.

Solution of the Mathematical Model

The dynamic mathematical model derived above is comprised of a large set of ordinary differential equations, with its size dependent on the number of volume elements chosen. Recycle causes the ODE's to be coupled. A computer program entitled DynAuto was developed to represent the model. DynAuto uses the ODE solver LSODE (Hindmarsh, 1980, 1983) that uses either a nonstiff or stiff (Gear) method. The model was written in FORTRAN and the simulations were performed using a IBM-PS/2 model 70 (20 MHz) with math coprocessor.

Simulation and Results

Some example simulations were performed to show the sensitivity of the mixing and model parameters and to compare with results from a commercial reactor. Simulations using a single volume element and with two elements were considered to study all the mixing parameters. The startup and grade change simulation and the gel formation simulations used a single volume element with no plug-flow segments. The reactor configuration and operating conditions chosen were (except as noted in the text for specific simulations):

Single volume element:

- Reaction temperature of 258°C
- About 21% conversion
- Pressure of 1,440 kg/cm^2
- Residence time of 37.6 s
- Monomer feed temperature of 40°C
- Using about 0.5 g/s Trigonox-B (di-tert-butyl peroxide) initiator. The initiator concentration is assumed to be equal in both the monomer rich and the polymer rich phases. The initiator decomposition rate constant was given by

$$kd = 8.843 \times 10^{12} \exp\left(-\frac{15{,}715.0}{T} - \frac{0.15811P}{T}\right) \qquad (7)$$

(s^{-1}). T is temperature in degrees Kelvin, P is pressure in kg/cm^2.

Two volume elements. The top element comprises approximately 45% of the total reactor volume:

- Reaction temperature of 258°C in the top element and 285°C in the second element
- Approximately 85% of the monomer feed is to the top element
- Other conditions as above

The kinetic parameters used for these simulations are given in Table 2. The propagation, termination and beta-scission rate constants and the activation energy for the transfer to polymer rate constant are as reported by Brandolin et al. (1988). The transfer to polymer rate constant reported by Brandolin et al. (1988) gave rise to a very large degree of long chain branching and thus was adjusted downward to give a more reasonable result for branching frequency and weight average molecular weight (Table 3). The transfer to polymer rate constant was later manipulated for the sensitivity analysis with respect to gel growth. The backbiting rate constant was selected to give the short chain branching frequency reported in Table 3.

Table 2. Kinetic Parameters Used for Example Simulations Except as Noted in the Text

Reaction	Frequency Factor	Activation Energy (cal/mol)
Propagation (cm^3/mol·s)	1.0×10^9	−5,245.0
Termination (cm^3/mol·s) $\phi_{tc} = 0.5$	3.0×10^{11}	−3,950.0
Backbiting (s^{-1})	3.27×10^5	−5,245.0
Beta scission (s^{-1})	7.3×10^6	−11,315.0
Transfer to polymer (cm^3/mol·s)	2.0×10^8	−9,500.0

Sensitivity analysis of the mixing parameters

Let us consider the sensitivity of the model predictions (steady state) to the mixing parameters, first for a single volume element, and then for two volume elements.

Single volume element

For a single volume element, there are two mixing parameters to be studied, the volume fraction of the CSTR component to the total volume element (θ_j) and the number of plug-flow segments in the volume element (N_p). The plots below show how the number of segments affects temperatures, initiator consumption, and molecular weight averages of the polymer produced. Figure 6 shows how the addition of the segments allows the gradual increase of segment temperatures, avoiding a sudden temperature rise from one volume element to the next. The outlet temperature from the reactor is nearly equal in all cases, but a smoother profile is generated by having more segments. Figure 7 presents the effect of the number of segments on initiator consumption, defined as the mass of initiator required to produce a certain amount of polymer. The initiator level is manipulated by the controller in order to maintain the temperature at the set point. More initiator is required as the

Table 3. Reasonable Molecular Weights and Branching Frequencies Used to Determine Transfer to Polymer and Backbiting Rate Constants for the Example Simulations

Quantity	Value	Units
No. avg. molec. wt.	16,000.0	g/mol
Wt. avg. molec. wt.	82,000.0	g/mol
Short chain branching freq.	21.8	Branches per 1,000 carbon atoms
Long chain branching freq.	0.48	Branches per 1,000 carbon atoms

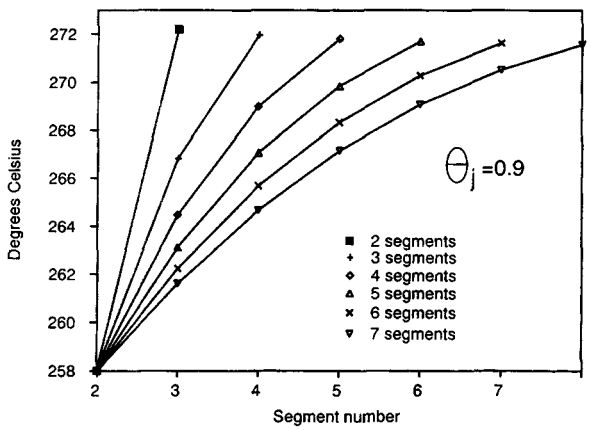

Figure 6. Effect of the number of segments on reaction temperatures in a single volume element.

The first segment is the CSTR segment and accounts for θ_j of the element volume.

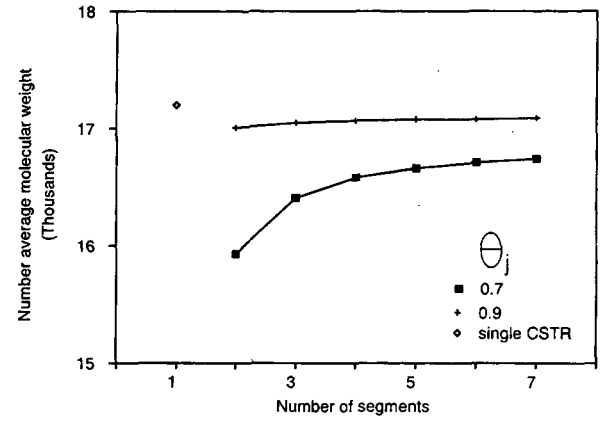

Figure 8. Effect of the number of segments on the number average molecular weight for a single volume element.

number of segments increases, especially for $\theta_j = 0.7$. This is in agreement with the observation that perfect mixing tends to consume less initiator than does poor mixing (van der Molen et al., 1982). Mixing becomes more segregated as the number of segments increases and as θ_j increases.

The effects of N_p and θ_j on the number of average molecular weights are shown in Figure 8. The number average molecular weight is highest for a single CSTR with no plug-flow segments and decreases as θ_j increases. Increasing the number of segments increases the number average molecular weight. The molecular weight averages are determined by the competition between propagation reaction and all other transfer (including transfer to polymer) and termination reactions. The relative rates of these reactions will change with temperature. The number average molecular weight decreases with increasing temperature, because the radical generation rate is higher, producing more polymer chains. In the single CSTR case all the polymer is produced at 258°C. When we have one plug-flow segment, θ_j of the reaction volume is at 258°C but the remainder of the volume is about 272°C (Figure 6), thus some of the polymer produced has a lower molecular weight. As the number of segments increases we have polymer produced at several intermediate temperatures between 258 and 272°C and thus the overall molecular weight increases.

The transfer to polymer has a higher activation energy than does propagation, and thus higher temperatures promote branching. Branching causes the molecular weight distribution to be broader as quantified by the polydispersity ($\overline{M}_w/\overline{M}_n$). Figure 9 shows the polydispersity decreasing with increasing numbers of segments and with increasing θ_j. This can be explained by the same argument as for the molecular weight averages.

Two volume elements

For multiple volume elements, there is an additional mixing parameter (recycle ratio) to be studied. For convenience, we use only two volume elements to analyze the effect of recycle ratio on temperatures, initiator consumption and number and weight average molecular weights. We shall study the first

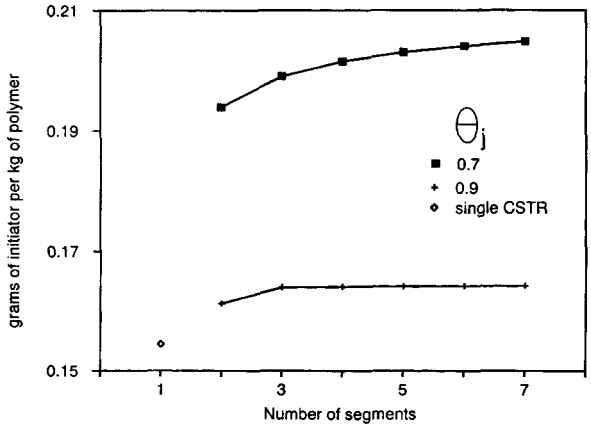

Figure 7. Effect of the number of segments on initiator consumption for a single volume element.

Initiator consumption is grams of initiator consumed per kilogram of polymer produced. The single CSTR has no plug-flow segments and $\theta_j = 1$.

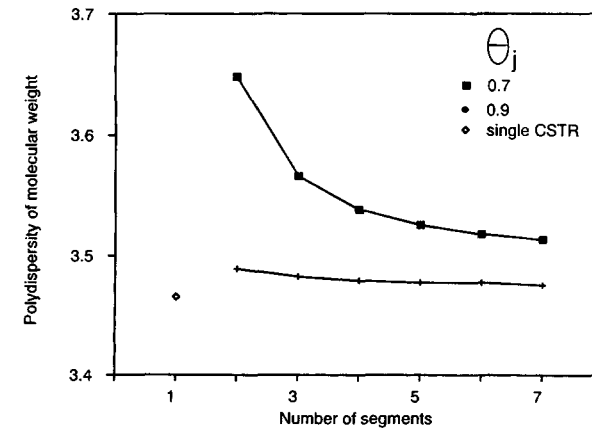

Figure 9. Effect of the number of segments on the polydispersity of molecular weight averages for a single volume element.

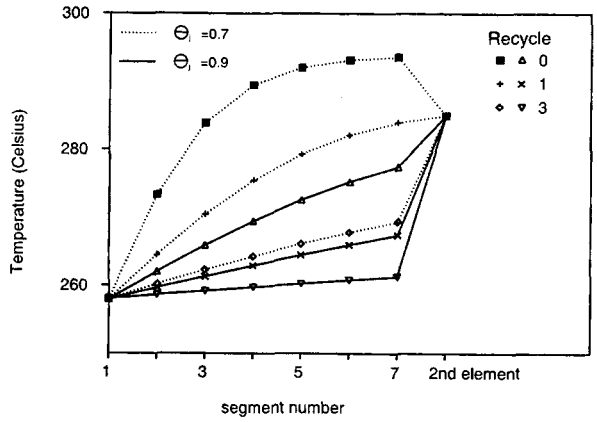

Figure 10. Mixing parameters for a two volume element system.

It shows the effect of recycle ratio, number of segments and CSTR volume fraction on temperatures in the first element. The second element temperature is held constant at 285°C.

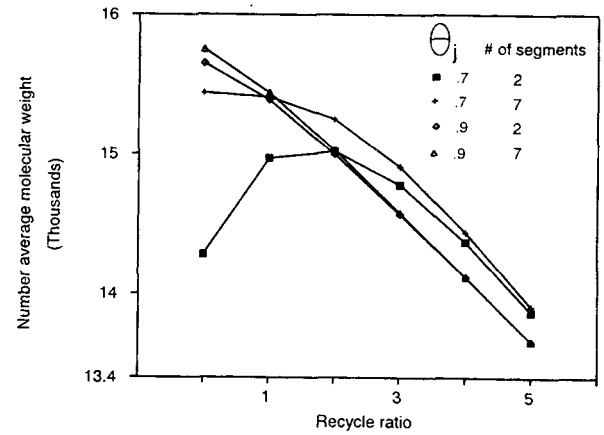

Figure 12. Mixing parameters for a two volume element system.

It shows the effects of recycle ratio, number of segments, and CSTR volume fraction on number average molecular weight of the polymer produced.

element and hold the second element temperature constant by manipulating the initiator flow to that element.

Figure 10 shows the effect of recycle ratio (q_j) on segment temperatures. As the recycle increases the temperature profiles become flatter. Increasing q_j reduces the single pass residence time and increases the mixing and in the limit the element behaves as a single CSTR as demonstrated by the nearly flat temperature profile at higher recycles. The $\theta_j = 0.7$, $q_j = 1$ gives a nice smooth temperature rise to the second volume element.

We have observed for the single volume element that the initiator consumption decreased with increasing mixing. Figure 11 shows that increasing the mixing, now by increasing the recycle, has a similar effect. The number of segments has a much smaller influence on initiator consumption than does the recycle rate or θ_j and the recycle swamps out the other variables at about $q_j = 4$ or 5.

The recycle influences the temperature profile and the monomer and initiator concentrations, which in turn affect the molecular weight averages. Figure 12 shows the relationship between number average molecular weight and recycle ratio.

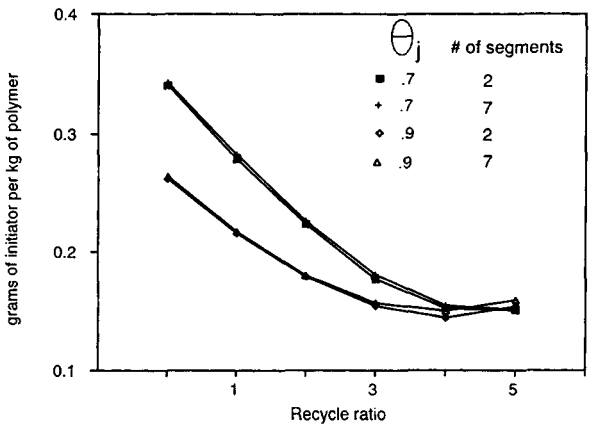

Figure 11. Mixing parameters for a two volume element system.

It shows the effects of recycle ratio, number of segments, and CSTR volume fraction on initiator consumption.

All curves collapse onto approximately the same line at recycle ratio near three indicating that beyond this point, N_p and θ_j have negligible effects on the number average molecular weight when compared to the effect of recycle. The number average molecular weight (for the $\theta_j = 0.7$, 2 segment case) passes through a maximum with increasing recycle. This can be explained by examining the initiator concentration in each volume segment for this case. The initiator concentration decreases with increasing recycle, in the CSTR segment of the first volume element (Figure 13). Since the number average molecular weight will grow smaller with elevated initiator concentrations, increasing the recycle increases the molecular weight of the polymer produced in this segment. However, at the same time, the initiator concentration, in the second element increases causing a reduction of the molecular weight of the polymer produced in this segment. The molecular weight of the final product is an average of the polymers produced in both seg-

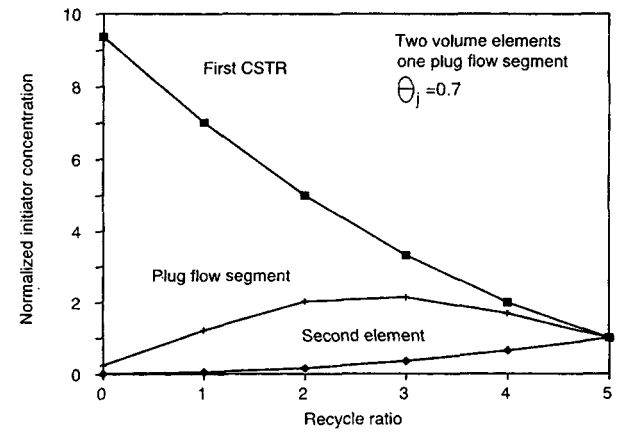

Figure 13. Effect of the recycle ratio on the initiator concentration in each segment for two volume elements.

One plug-flow segment in the first element, θ_j = 0.7. The concentrations for each segment are normalized by division by the segment concentration at a recycle ratio of five.

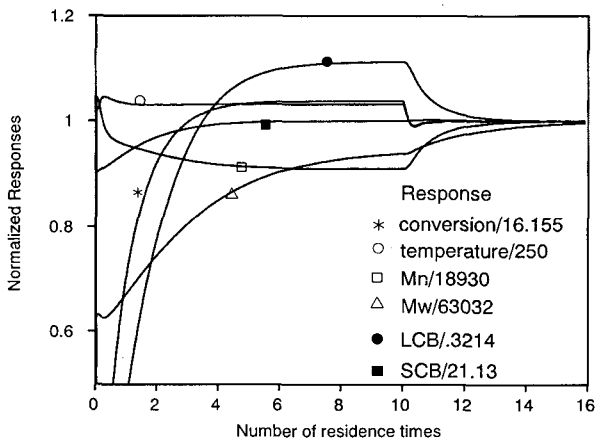

Figure 14. Dynamic response of a single CSTR during start-up from pure ethylene, initially at 255°C.

The reactor set point is changed to 250°C after about 10 residence times to simulate a grade change.

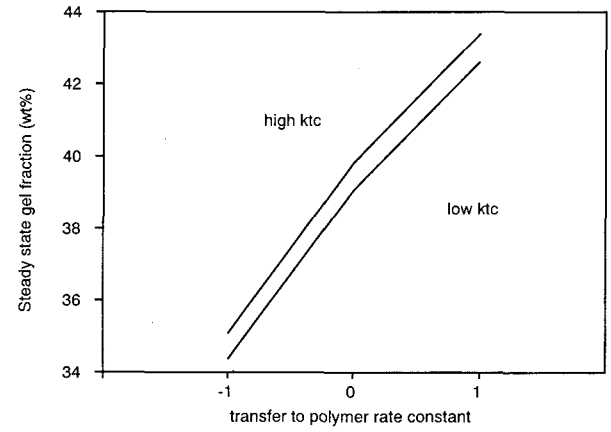

Figure 15. Gel fraction at steady state as a function of termination by combination and transfer to polymer rate.

Single CSTR, temperature fixed at 258°C.

ments, and thus M_n passes through a maximum because of the two competing effects.

Startup and grade changes

During real plant operation, the procedure used to switch from one polymer grade to another is critical because it often leads to off specification material produced during the transition period. Knowledge of dynamic responses of the process variables is essential to promote appropriate control actions and grade transition policies. The dynamic response of a single volume element (1 segment) at startup and for one grade change is shown in Figure 14. Initial conditions are that the reactor is full of pure ethylene at 255°C. A grade change is implemented near 10 residence times by changing the set point temperature to 250°C. The responses are normalized by dividing each individual response by its final value so that they may be plotted on the same axes for comparison. Notice that the temperature and conversion of monomer reach steady state quickly, as influenced by the controller. However, the molecular properties, especially the weight average molecular weight, take much longer to reach the steady state. The short chain branching frequency does not change with the change in temperature since we have specified that the activation energy for backbiting is the same as that for propagation.

Gel formation

It has been reported (Cozewith et al., 1979) that under some circumstances a steady state cannot be reached in a continuous flow stirred tank reactor for crosslinking systems. However, the molecular weight equations that they use describe the entire polymer population before the gel point. They observe that there are cases where the steady state cannot be reached without the higher molecular weight moments going to infinity, indicating the gel point. Our work agrees with this, however, we have also included the equations to describe the sol polymer and the gel fraction after the gel point and a steady state can be reached after the gel point. All of the sol molecular weight moments remain finite. In fact the polydispersity actually decreases after the gel point, since the gel preferentially consumes the longer chains.

Two important kinetic parameters influencing the mass of gel in the reactor, are the transfer to polymer rate constant (k_{fp}) and the fraction of termination by combination, ϕ_{tc}. Figure 15 shows the influence of transfer to polymer and termination by combination rate constants on the steady-state gel fraction, for the levels specified in Table 4. As transfer to polymer, and the fraction of termination by combination increase, the steady-state gel fraction also increases. If termination is all by disproportionation, then no gel should be formed even in the presence of transfer to polymer reactions (Tobita and Hamielec, 1989b).

In order to study the gel formation dynamics, a transient was induced from a steady-state gel fraction value of near 50% and the response monitored for two different k_{fp} and ϕ_{tc} values. This initial gel level is quite high, but was chosen to better illustrate the behavior. The energy balance equations were not solved. The initiator flow and the temperature were fixed to isolate the molecular weight behavior from the dynamic temperature response. The results are shown in Figure 16. The gel levels may oscillate before steady state is reached and the transients are larger and longer lived if the parameters influencing the rate of gel formation (k_{fp} and ϕ_{tc}) are lower. The molecular weight averages and the gel fractions are also correlated. The rate of gel growth increases as the molecular weight averages increase, since larger molecules are added to the gel for each termination by combination reaction. However, gel preferentially consumes larger molecules, because it is more probable to encounter a radical center in a large chain than on a small one. Thus an increase in molecular weight causes gel to grow

Table 4. Levels of the Kinetic Parameters Used for the Gel Study

	Level		
Variable	−1	0	1
k_{fp}/k_p	1.09×10^{-2}	1.45×10^{-2}	1.82×10^{-2}
ϕ_{tc}	0.5	0.75	1.0

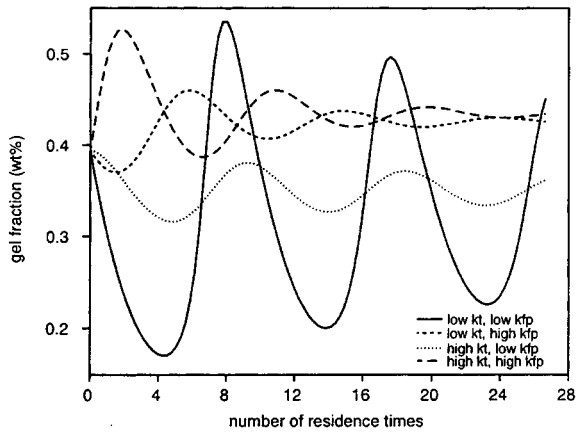

Figure 16. Effects of termination by combination and transfer to polymer rates on the transient gel levels.

Single CSTR, temperature fixed at 258°C.

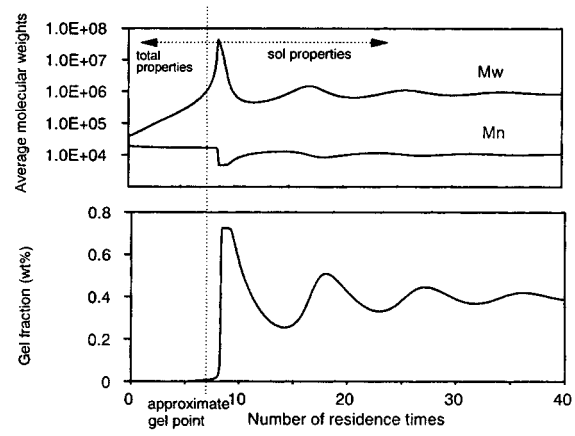

Figure 18. Dynamic behavior of the molecular weight averages and the gel fraction in the pregel and post gel region.

Start-up from a reactor full of pure ethylene at 258°C. High values of the transfer to polymer and termination by combination rate constants were used.

faster, then the growing gel consumes the larger chains, reducing the molecular weight averages. Finally, clumps of gel are allowed to flow out of the reactor, reducing the gel fraction, and hence providing the opportunity for the molecular weight to grow again. This cycle is presented in Figure 17. The molecular weight averages, especially the number average, lead the gel fraction. Larger and longer lived oscillations were observed at lower values of k_{fp} and ϕ_{tc}. Lower values of these parameters cause lower gel growth rates, and thus the molecular weight averages are allowed to grow to much larger values. When the molecular weight averages are high, the gel growth rate becomes quite large, and a huge oscillation is started quickly driving the gel level up and the molecular weights down. At higher values of k_{fp} and ϕ_{tc} the gel growth is faster and the high molecular weight averages are avoided. The oscillation in gel fraction still needs to be verified by experiment.

A second case, reactor start-up, was simulated. The reactor was initially full of pure ethylene at 258°C and then the monomer and initiator flows were started and the reaction allowed to come to steady state. In this case high values of k_{fp} and δ_{tc} were selected to promote gel formation. Figure 18 shows the molecular weight averages and the gel fraction behavior with time. In the pregel region the molecular weights shown apply to all the polymer but in the post gel region the molecular weight averages only describe the sol polymer. Initially there is no gel in the reactor and the molecular weight averages grow and the polydispersity increases. When the gel point is reached (as indicated in our simulation by a polydispersity greater than about 20) the gel slowly begins to grow, and the molecular weight averages continue to increase. However, after a brief time, the gel fraction quickly grows and the molecular weight averages and the polydispersity of the sol polymer sharply decrease. The system gradually oscillates to a steady state after about 40 residence times.

We have studied the influence of the kinetic parameters k_{fp} and ϕ_{tc} by setting them to arbitrary values. It should be pointed out that these values will be influenced by temperature and pressure and thus are functions of the operating conditions. Moreover, the presence and the concentration of the polymer rich phase is also a function of temperature and pressure, and must also influence gel formation. Increasing the temperature and the pressure decreases the weight fraction of polymer in the polymer rich phase and thus should also decrease the tendency to form gel polymer.

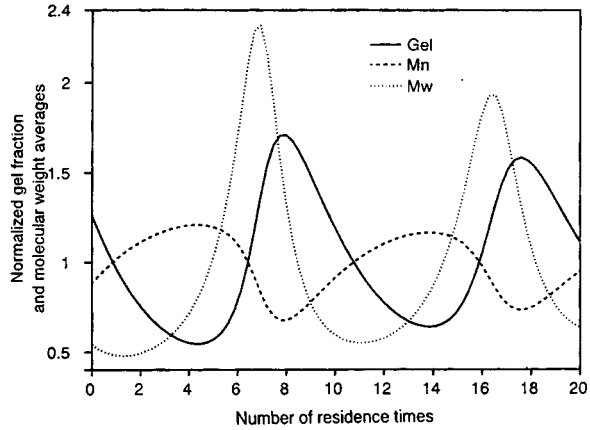

Figure 17. Dynamic relationship between the sol molecular weight averages and the gel fraction.

Single CSTR, temperature fixed at 258°C.

Comparisons with industrial data

Actual industrial production recipes were used for simulation to test part of the model by comparing the observed steady-state values with those predicted from the model for monomer conversion, copolymer composition, initiator flow rates and temperature profile along the reactor. Unfortunately we do not have measurements of molecular weight branching frequencies or gel fractions, and thus cannot make comparisons with these quantities. Therefore, this section only tests the mixing model the parts of the model related to the rate of polymerization and heat generation rates.

The set of model parameters used for the previous simulations did not completely represent the industrial data so a

Table 5. Comparison Between Industrial Plant Data and the Model Predictions

Response	Resin 1 (Homopolymer)			Resin 2 (Copolymer)		
	Pred.	Obs.	Error (%)	Pred.	Obs.	Error (%)
Normalized temperature						
Level 9 (top)	0.9908	0.9923	−0.15	0.726	0.726	0
Level 8	0.9908	0.9923	−0.15	0.726	0.726	0
Level 7	0.9935	0.9923	0.12	0.726	0.726	0
Level 6	0.9935	0.9923	0.12	0.726	0.726	0
Level 5	1	0.9923	0.78	0.836	0.827	1.09
Level 4	1	1	0	0.937	0.907	3.31
Level 3	1	1	0	0.977	0.968	0.93
Level 2	1	1	0	0.996	0.992	0.40
Level 1 (bottom)	1	1	0	0.996	1	−0.40
Total initiator flow rate (g/s)	0.54	0.55	−1.82	3.20	2.84	12.68
Total conversion	0.178	0.169	5.33	0.164	0.153	7.19
Comonomer composition (wt. % monomer 2)	—	—	—	4.0	4.2	−4.76

new set were fit to the data. However these kinetic parameters and the process information used to run the model must remain proprietary. The initiator decomposition rate constants used were as reported by the initiator suppliers. The rate constants for propagation and termination were chosen to fit all of the polymerization rate data. The rate constants for transfer to modifier, beta scission, and transfer to polymer were not needed to describe these observations, since we have no molecular weight data. The mixing parameters (number of elements, and recycles) were chosen to match the temperature profiles and initiator flows for specific recipes. Table 5 summarizes the results obtained for both ethylene homopolymer and ethylene-vinyl acetate copolymer.

The results obtained from the model are quite good in comparison with the actual plant data. The largest relative error of the predicted values was less than thirteen percent for initiator flow rate, and all model responses are within the measurement error of the data collected.

Conclusions

We have endeavored to construct a comprehensive model to describe the high-pressure homo- and copolymerization of ethylene in autoclave type reactors. This model accounts for the important chemical reactions, the mixing pattern in the vessel, and the two-phase kinetics. It also incorporates the mass and energy balances on the vessel, as well as the temperature controller equations. The model predicts polymer properties such as composition, molecular weight, branching frequencies and gel content.

The model was fit to both homopolymer and copolymer recipes for initiator flow rates and temperature profiles. The fit was quite adequate for steady-state conditions. No dynamic data are currently available to test the transient behavior. More data are needed to verify the model predictions for the molecular properties.

To our knowledge, no one has previously presented predictions of gel content for this flow system. The gel content shows oscillations in the transients, but steady state values may be reached which are insensitive to the initial conditions.

Acknowledgments

The authors wish to acknowledge Poliolefinas S. A. for financial support for this project. Thanks to Mr. R. C. M. Zabisky and A. B. M. de Carvalho for their encouragement and assistance and to Mr. P. R. Bellotti for his work in developing the simplified thermodynamic correlation.

Notation

Cp = heat capacity of mixture, cal/g·°C
C_{pi} = dimensionless group for molecular weight calculations related to transfer to polymer
f = initiator efficiency
f_1, f_2 = monomer composition (mole fraction of monomers 1 and 2)
F_1, F_2 = instantaneous copolymer compositions (mole fraction of monomers 1 and 2 bound as polymer)
$\bar{F}_1, \bar{F}_2$ = accumulated copolymer compositions (mole fraction of monomers 1 and 2 bound as polymer)
F = molar flow rate, mol/s
F_I = molar initiator flow rate, mol/s
F_r = molar recycle flow rate, mol/s
H = change in enthalpy of the reactor contents from the reference conditions, cal
ΔH = heat of polymerization, cal/mol
I = initiator species
k_b = rate constant for backbiting reaction, s^{-1}
k_d = rate constant for initiator decomposition reaction, s^{-1}
k_{fm} = rate constant for transfer to monomer reaction, cm^3/mol·s
k_{fp} = rate constant for transfer to polymer reaction, cm^3/mol·s
k_{fts} = rate constant for transfer to modifier reaction, cm^3/mol·s
k_p = rate constant for propagation reaction, cm^3/mol·s
k_{pts} = rate constant for modifier incorporation reaction, cm^3/mol·s
k_{tc} = rate constant for termination by combination reaction, cm^3/mol·s
k_{tcsg} = rate constant for termination by combination reaction between one sol radical and one gel radical, cm^3/mol·s
k_{tcss} = rate constant for termination by combination reaction between two radicals, cm^3/mol·s
k_{td} = rate constant for termination by disproportionation reaction, cm^3/mol·s
k_{tdsg} = rate constant for termination by disproportionation reaction between one sol radical and one gel radical, cm^3/mol·s
k_{tdss} = rate constant for termination by disproportionation reaction between two sol radicals, cm^3/mol·s
K_I = partition coefficient for initiator (mol/cm^3 in monomer rich phase:mol/cm^3 in polymer rich phase)
K_p = proportional gain for the controller, g/s·°C

K_{TS} = partition coefficient for modifier (mol/cm^3 in monomer rich phase:mol/cm^3 in polymer rich phase)
LCB = moles of long chain branches
m_1, m_2 = molecular weight of monomers, g/mol
M = monomer species
M_g = moles of monomer units bound as gel polymer
N_p = number of plug flow segments in a volume element
N_v = number of volume elements in the reactor
P_1, P_2 = moles of monomer units bound in the polymer
Q = volumetric flow rate, cm^3/s
Q_i = ith moment of the polymer distribution, mol/cm^3
Q_r = volumetric recycle flow rate, cm^3
q_j = recycle ratio at volume element j
R = radical species
r_1, r_2 = reactivity ratios
r, R_p = rate of reaction, mol/cm^3·s
r_n = number average chain length
r_w = weight average chain length
SCB = moles of short chain branches
TS = modifier
T_{set} = set point temperature, °C
V_j = volume of a single volume element, cm^3
$V_{j,L}$, V_s = volume of a segment, cm^3
V_m = volume of the monomer rich phase, cm^3
V_{out} = volumetric outflow rate from a segment, cm^3·s
V_p = volume of the polymer rich phase, cm^3
V_T = total volume of the reactor, cm^3
W_p = mass of polymer in the polymer rich phase, g
W_f = weight fraction of polymer in the polymer rich phase
X_1, X_2, X_3 = normalized variables for temperature, pressure and weight average molecular weight respectively
$[X_k]$ = concentration of species X_k, mol/cm^3
Y_i = ith moment of the radical distribution, mol/cm^3

Greek letters

β, τ = dimensionless group for molecular weight calculations
τ_I = integral time constant for the controller, s
τ_D = derivative time constant for the controller, s
ϕ_1, ϕ_2 = mole fraction of polymer radicals
Φ_m = ratio of the mass of monomer in polymer rich phase to the mass of polymer in the polymer rich phase
ϕ_{ic} = fraction of total termination by combination
θ_j = volume fraction of the CSTR component to the total volume element j
ρ = density, g/cm^3
λ_L = number of long chain branches per 1,000 carbon atoms
λ_s = number of short chain branches per 1,000 carbon atoms

Subscripts

g = related to gel polymer
m = related to monomer rich phase
p = related to polymer rich phase
r = related to recycle
TS = related to modifier
1,2 = related to monomers 1 and 2

Literature Cited

Bogdanovic, V., and J. Srdanovic, "Differences Between Low Density Polyethylenes Synthesized at Homogeneous and Heterogeneous Reaction Conditions," *J. Appl. Polym. Sci.*, **31**, 1143 (1986).

Box, G. E. P., W. G. Hunter, and J. S. Hunter, *Statistics for Experimenters*, Wiley, New York, p. 323 (1978).

Brandolin, A., N. J. Capiati, J. N. Farber, and E. M. Vales, "Mathematical Model for High-Pressure Tubular Reactor for Ethylene Polymerization," *Ind. Eng. Chem. Res.*, **27**, 784 (1988).

Cozewith, C., W. W. Graessley, and G. Ver Strate, "Polymer Crosslinking in Continuous Flow Stirred Reactors," *Chem. Eng. Sci.*, **34**, 245 (1979).

Donati, G., M. Gramondo, E. Langianni, and L. Marini, "Low Density Polyethylene in Vessel Reactors," *Ing. Chim. Ital.*, **17**, 88 (1981).

Georgakis, C., and L. Marini, "The Effect of Mixing on Steady-State and Stability Characteristics of Low Density Polyethylene Vessel Reactors," *ACS Symp. Ser.*, **196**, Chemical Reaction Engineering, Boston, pp. 591-602 (1982).

Hamielec, A. E., J. F. MacGregor, and A. Penlidis, "Multicomponent Free-Radical Polymerization in Batch, Semi-Batch and Continuous Reactors," *Makromol. Chem. Macromol. Symp.*, **10/11**, pp. 521-570 (1987).

Hindmarsh, A. C., "LSODE and LSODI, Two New Initial Value Ordinary Differential Equation Solvers," *ACM-Signum Newsletter*, **15**(4), 10 (1980).

Hindmarsh, A. C., "ODEPAC, A Systematized Collection of ODE Solvers," *Scientific Computing*, S. Stepleman et al., eds., (Volume 1 of *IMACS Transactions on Scientific Computation*) North-Holland, Amsterdam, pp. 55-64 (1983) .

Hulburt, H. M., and S. Katz, "Some Problems in Particle Technology, A Statistical Mechanical Formulation," *Chem. Eng. Sci.*, **19**, 555 (1964).

Marini, L., and C. Georgakis, "Low Density Polyethylene Vessel Reactors," *AIChE J.*, **30**, 401 (1984)

PFLASH documentation, "Continuous Thermodynamics and Phase Equilibria in Polymeric Systems," Poliolefinas software (1988).

Sako, T., A. Wu, and J. M. Prausnitz, "A Cubic Equation of State for High Pressure Phase Equilibria of Mixtures Containing Polymers and Volatile Fluids," *J. Appl. Polym. Sci.*, **38**, 1839 (1989).

Tobita, H., and A. E. Hamielec, "Crosslinking Kinetics in Free Radical Copolymerization," *Polymer Reaction Engineering*, 3rd International Workshop on Polymer Reaction Engineering, VCH Publishers, N.Y., pp. 43-83 (1989b).

Tobita, H., and A. E. Hamielec, "Modelling of Network Formation in Free Radical Polymerization," *Macromolecules*, **22**, 3098 (1989a).

van der Molen, T., A. Keonen, H. Oosterwijk, and H. van der Bend, "Light-Off Temperature and Consumption of 16 Initiators in LDPE Production," *Ing. Chim. Ital.*, **18**, 7 (1982).

Zabisky, R. C. M., W. M. Chan, P. E. Gloor, and A. E. Hamielec, "A Kinetic Model for Olefin Polymerization in High-Pressure Tubular Reactors: A Review and Update," *Polymer*, **33**, 2243 (1992).

Appendix

Mass and energy balance equations

Given the mixing model, one can construct the mathematical model by writing the mass and energy balances for a single volume segment. The mass balance for a species in a volume segment will, in general, have the form:

accumulation in volume segment
= outflow from previous segment
+ feed to segment
+ recycle from next element
− outflow to next segment
− recycle to previous element
+ net generation by reaction (4)

Mathematically, for any species X_k

$$\frac{dX_{k,(j,L)}}{dt} = F^{x_k}_{j,L-1} + F^{x_k}_{f,(j,L)} + F^{x_k}_{r,(j+1,L)} - F^{x_k}_{j,L} - F^{x_k}_{r,(j,L)} + r^{x_k}_{j,L} V_{j,L} \tag{A1}$$

where
X_k = moles of species x_k
F^{x_k} = molar flow rate of species x_k
$F^{x_k}_r$ = molar recycle flow rate of species x_k
r^{x_k} = rate of reaction to generate species x_k

j refers to the volume element, and L refers to the volume segment. Note that from our mixing model:

$$F_{j,1} = F_{j-1,N_p+1} \tag{A2}$$

$$F_{f,(j,1)} = F_{f_j} \tag{A3}$$

For the plug-flow segments ($L > 1$) there is no feed or recycle

$$F_{f,(j,L)} = F_{r,(j,L)} = 0 \tag{A4}$$

It is also true that in a CSTR, the following relation holds:

$$F^{x_k}_{j,L} = [X_k]_{(j,L)} \frac{V_{\text{out}(j,L)}}{V_{j,L}} \tag{A5}$$

where V_{out} is the volumetric outflow rate. Defining the recycle ratio at volume element j as q_j,

$$q_j = \frac{Q_{r,(j,1)}}{\sum_{k=1}^{N_c} (Q^{M_1}_{f_k} + Q^{M_2}_{f_k})} \tag{A6}$$

where Q_r is the volumetric recycle flow rate and $Q^{M_1}_{f_k}$ and $Q^{M_2}_{f_k}$ are the volumetric flow rates of monomer 1 and 2 in the f_k stream. The volumetric feed rates of monomer one and two are given by

$$Q^{M_1}_{f_k} = \frac{F^{M_1}_{f_k}}{[M_1]_{f_k}} \qquad Q^{M_2}_{f_k} = \frac{F^{M_2}_{f_k}}{[M_2]_{f_k}} \tag{A7}$$

so the recycle flow rate will be given by

$$Q_{r,(j,1)} = q_j \sum_{k=1}^{N_c} \left(\frac{F^{M_1}_{f_k}}{[M_1]_{f_k}} + \frac{F^{M_2}_{f_k}}{[M_2]_{f_k}} \right) \tag{A8}$$

The recycle molar flow rate for each species is then given by

$$F^{x_k}_{r,(j,1)} = [X_k]_{j,1} Q_{r,(j,1)} \tag{A9}$$

q_j is a parameter to be estimated, and is zero for all plug-flow volume segments.

To determine $V_{\text{out}(j,L)}$, assume that volumes are additive and the reaction mixture is essentially monomer and polymer

$$V_{\text{out}(j,L)} = \sigma_{M_1} m_1 + \sigma_{M_2} m_2 + \sigma_{P_1} m_1 + \sigma_{P_2} m_2 \tag{A10}$$

where

$$\sigma_{M_1} = \frac{F^{M_1}_{j,L-1} + F^{M_1}_{f,(j,L)} + Q_{r,(j+1,L)}[M_1]_{j+1,L} - Q_{r,(j,L)}[M_1]_{j,L} + r^{M_1}_{j,L} V_{j,L}}{\rho^{M_1}_{j,L}} \tag{A11}$$

$$\sigma_{M_2} = \frac{F^{M_2}_{j,L-1} + F^{M_2}_{f,(j,L)} + Q_{r,(j+1,L)}[M_2]_{j+1,L} - Q_{r,(j,L)}[M_2]_{j,L} + r^{M_2}_{j,L} V_{j,L}}{\rho^{M_2}_{j,L}} \tag{A12}$$

$$\sigma_{P_1} = \frac{F^{P_1}_{j,L-1} + Q_{r,(j+1,L)}[P_1]_{j+1,L} - Q_{r,(j,L)}[P_1]_{j,L} + r^{P_1}_{j,L} V_{j,L}}{\rho^{P}_{j,L}} \tag{A13}$$

$$\sigma_{P_2} = \frac{F^{P_2}_{j,L-1} + Q_{r,(j+1,L)}[P_2]_{j+1,L} - Q_{r,(j,L)}[P_2]_{j,L} + r^{P_2}_{j,L} V_{j,L}}{\rho^{P}_{j,L}} \tag{A14}$$

and

m_1 = molecular weight of monomer type 1, g/mol
m_2 = molecular weight of monomer type 2, g/mol
ρ^{M_1} = density of monomer 1, g/cm^3
ρ^{M_2} = density of monomer 2, g/cm^3
ρ^{P} = density of polymer, g/cm^3

The rates of reactions $r^{M_1}_{j,L}$, $r^{M_2}_{j,L}$, $r^{P_1}_{j,L}$ and $r^{P_2}_{j,L}$ will be derived in the next section.

We can solve the set of ODE for $X_{k,(j,L)}$ of the form,

$$V_{j,L} \frac{d[X_k]_{j,L}}{dt} = F^{x_k}_{j,L-1} + F^{x_k}_{f,(j,L)} + Q_{r,(j+1,L)}[X_k]_{j+1,L} - (Q_{r,(j,L)} + V_{\text{out}(j,L)})[X_k]_{j,L} + r^{x_k}_{j,L} V_{j,L} \tag{A15}$$

Depending upon the segment type, there may or may not be fresh feeds or recycles. For simplicity, we are adopting the following notation in our subsequent model development.

$$(\text{inflow} - \text{outflow})^{x_k}_{j,L} = F^{x_k}_{j,L-1} + F^{x_k}_{f,(j,L)} + Q_{r,(j+1,L)}[X_k]_{j+1,L} - (Q_{r,(j,L)} + V_{\text{out}(j,L)})[X_k]_{j,L} \tag{A16}$$

Two phase kinetics

Let Φ_m be the ratio of the mass of monomer to the mass of polymer, both in the polymer rich phase. This quantity can be calculated from:

$$\Phi_m = \frac{1}{W_t} - 1 \tag{A17}$$

where W_t is the mass fraction of polymer in the polymer rich phase given by Eq. 3. Defining W_p as the mass of polymer in the polymer rich phase, one can evaluate the volume of the polymer rich phase (swollen with monomer) as:

$$V_p = \left(\frac{m_1 f_1}{\rho_1} + \frac{m_2 f_2}{\rho_2} \right) \left(\frac{W_p \Phi_m}{m_1 f_1 + m_2 f_2} \right) + \frac{W_p}{\rho_p} \tag{A18}$$

$$W_p = m_1 P_1 + m_2 P_2 \tag{A19}$$

where f_1 and f_2 are mole fractions of monomer 1 and 2; m_1 and m_2 are the molecular weights of monomer 1 and 2; ρ_1, ρ_2 and ρ_p refer to density of monomer 1, monomer 2 and polymer respectively; P_1 and P_2 are monomer 1 units and monomer 2 units bound as polymer. This assumes that the volumes are additive. The monomer rich phase volume is given by:

$$V_m = V_s - V_p \tag{A20}$$

where V_s is the volume of the segment.

Now that we have expressions to calculate V_m and V_p, we are now able to derive mass balance equations for each species in an arbitrary volume segment (j, L). Firstly, we assume the initiator and the modifier to partition according to:

$$\frac{[I]_m}{[I]_p} = K_I \tag{A21}$$

$$\frac{[TS]_m}{[TS]_p} = K_{TS} \tag{A22}$$

K_I and K_{TS} need not be identical for all initiator or modifier types. In our simulations both K_I and K_{TS} were assumed to be unity. From the mass balances and the partition coefficients, one can calculate the concentration of initiator and modifier in each phase as:

$$[I]_p = \frac{[I]_{\text{total}} V_s}{K_I V_m + V_p}$$
$$[TS]_p = \frac{[TS]_{\text{total}} V_s}{K_{TS} V_m + V_p} \tag{A23}$$

If the stationary state hypothesis (SSH) is adopted, then we can calculate the radical concentrations in each phase. For the pregel region

$$[R]_m = \left(\frac{2fk_d[I]_m}{k_t}\right)^{1/2}$$
$$[R]_p = \left(\frac{2fk_d[I]_p}{k_t}\right)^{1/2} \tag{A24}$$

where $k_t = k_{tc} + k_{td}$. In the postgel region, the polymer rich phase is composed of sol plus gel. The monomer rich phase radical concentration is unchanged and the polymer phase radical concentrations are given by these two simultaneous algebraic equations:

$$[R]_g = \frac{k_{fp}[M_g][R]_p}{k_{fm}[M]_p + k_\beta + (k_{tcsg} + k_{tdsg})[R]_p + k_{fp}[Q_1]_p + k_{fts}[TS]_p} \tag{A26}$$

$$0 = (k_{tcss} + k_{tdss})[R]_p^2 + \{k_{fp}[M_g] + (k_{tcsg} + k_{tdsg})[R]_g\}[R]_p - \{2fk_d[I]_p + k_{fm}[M]_p[R]_g + k_{fts}[TS]_p[R]_g + k_{fp}[R]_g[Q_1]_p\} \tag{A27}$$

where $[M_g]$ denotes the moles of monomer units bound in the gel per unit of volume; $[R]_p$ is the sol radical concentration; $[Q_1]_p$ represents the first polymer moment in the sol; and the subscript 'sg' in the termination rate constants denote sol-gel. Note that we have assumed that $k_{tcss} = k_{tc}$, and $k_{tdss} = k_{td}$.

A balance on initiator and monomer types 1 and 2 gives:

$$V_s \frac{d[I]_{\text{total}}}{dt} = (\text{inflow} - \text{outflow})_{j,L}^{I} - k_d\{[I]_m V_m + [I]_p V_p\} \tag{A28}$$

$$V_s \frac{d[M_1]}{dt} = (\text{inflow} - \text{outflow})_{j,L}^{M_1} - k_{p11}\{[M_1]_m\phi_1[R]_m V_m + [M_1]_p\phi_1([R]_p + [R]_g)V_p\} - k_{p21}\{[M_1]_m\phi_2[R]_m V_m + [M_1]_p\phi_2([R]_p + [R]_g)V_p\} \tag{A29}$$

$$V_s \frac{d[M_2]}{dt} = (\text{inflow} - \text{outflow})_{j,L}^{M_2} - k_{p12}\{[M_2]_m\phi_1[R]_m V_m + [M_2]_p\phi_1([R]_p + [R]_g)V_p\} - k_{p22}\{[M_2]_m\phi_2[R]_m V_m + [M_2]_p\phi_2([R]_p + [R]_g)V_p\} \tag{A30}$$

The concentrations of monomer in the polymer and monomer rich phases are given by:

$$[M_1]_p = \frac{f_1 W_p \Phi_m}{V_p(m_1 f_1 + m_2 f_2)} \tag{A31}$$

$$[M_2]_p = \frac{f_2 W_p \Phi_m}{V_p(m_1 f_1 + m_2 f_2)} \tag{A32}$$

$$[M_1]_m = \frac{V_s[M_1] - [M_1]_p[V_p]}{V_m} \tag{A33}$$

$$[M_2]_m = \frac{V_s[M_2] - [M_2]_p[V_p]}{V_m} \tag{A34}$$

Similar balances can be made to find the moles of each monomer bound as polymer and the modifier in the reactor.

$$V_s \frac{d[P_1]}{dt} = (\text{inflow} - \text{outflow})_{j,L}^{P_1} + k_{p11}\{[M_1]_m\phi_1[R]_m V_m + [M_1]_p\phi_1([R]_p + [R]_g)V_p\} + k_{p21}\{[M_1]_m\phi_2[R]_m V_m + [M_1]_p\phi_2([R]_p + [R]_g)V_p\} \tag{A35}$$

$$V_s \frac{d[P_2]}{dt} = (\text{inflow} - \text{outflow})_{j,L}^{P_2} - k_{p12}\{[M_2]_m\phi_1[R]_m V_m + [M_2]_p\phi_1([R]_p + [R]_g)V_p\} + k_{p22}\{[M_2]_m\phi_2[R]_m V_m + [M_2]_p\phi_2([R]_p + [R]_g)V_p\} \tag{A36}$$

$$V_s \frac{d[TS]}{dt} = (\text{inflow} - \text{outflow})_{j,L}^{TS} - k_{fts}\{[R]_m[TS]_m V_m + ([R]_p + [R]_g)[TS]_p V_p\} - k_{pts}\{[R]_m[TS]_m V_m + ([R]_p + [R]_g)[TS]_p V_p\} \tag{A37}$$

Molecular weight and moment equations

We are using the method of moments to find the molecular weight averages. r_n and r_w are the number and weight average chain lengths and Q_0, Q_1, Q_2 are the leading moments of the molecular weight distribution.

$$r_n = \frac{[Q_1]}{[Q_0]} \qquad r_w = \frac{[Q_2]}{[Q_1]} \tag{A38}$$

The leading moments for radical and polymer chain length distribution for each phase are derived below. By definition, the moments of the dead polymer and macroradical distribution are:

$$[Q_i] = \sum_{r=2}^{\infty} r^i [P(r)] \tag{A39}$$

$$[Y_i] = \sum_{r=1}^{\infty} r^i [R(r)] \tag{A40}$$

Notice that

$$[Y_{i+1}] >> [Y_i] >> [Y_{i-1}]$$
$$[Q_{i+1}] >> [Q_i] >> [Q_{i-1}]$$
$$[Q_i] >> [Y_i]$$

and we will take advantage of these inequalities to simplify our expressions whenever is possible. We will also neglect the term $2fk_d[I]$ where its value is insignificant as compared to other terms.

Firstly consider the pregel region. The radical moments are given by:

$$[Y_0]_m = [R]_m = \left(\frac{2fk_d[I]_m}{k_t}\right)^{0.5} \tag{A41}$$

$$[Y_0]_p = [R]_p = \left(\frac{2fk_d[I]_p}{k_t}\right)^{0.5} \tag{A42}$$

$$[Y_1]_m = \frac{[Y_0]_m}{\tau_m + \beta_m} \tag{A43}$$

$$[Y_1]_p = \frac{(1 + C_{p2})[Y_0]_p}{\tau_p + \beta_p + C_{p1}} \tag{A44}$$

$$[Y_2]_m = \frac{2[Y_0]_m}{(\tau_m + \beta_m)^2} \tag{A45}$$

$$[Y_2]_p = \frac{2[Y_1]_p + C_{p3}[Y_0]_p}{\tau_p + \beta_p + C_{p1}} \tag{A46}$$

where

$$\tau_m = \frac{k_{fm}[M]_m + k_{fts}[TS]_m + k_\beta + k_{td}[Y_0]_m}{k_p[M]_m} \tag{A47}$$

$$\tau_p = \frac{k_{fm}[M]_p + k_{fts}[TS]_p + k_\beta + k_{td}[Y_0]_p}{k_p[M]_p} \tag{A48}$$

$$\beta_m = \frac{k_{tc}[Y_0]_m}{k_p[M]_m} \tag{A49}$$

$$\beta_p = \frac{k_{tc}[Y_0]_p}{k_p[M]_p} \tag{A50}$$

$$C_{pi} = \frac{k_{fp}[Q_i]_p}{k_p[M]_p} \tag{A51}$$

The polymer moments are given by

$$V_s \frac{d[Q_0]}{dt} = (\text{inflow} - \text{outflow})^{Q_0}_{j,L} + \left(\tau_m + \frac{\beta_m}{2}\right) k_p[M]_m[Y_0]_m V_m + \left(\tau_p + \frac{\beta_p}{2}\right) k_p[M]_p[Y_0]_p V_p \tag{A52}$$

$$[Q_1] = [P_1] + [P_2] \tag{A53}$$

$$V_s \frac{d[Q_2]}{dt} = \left[\frac{2}{\tau_m + \beta_m} + \frac{\beta_m}{(\tau_m + \beta_m)^2}\right] k_p[M]_m[Y_0]_m V_m + \left[\frac{2(1 + C_{p2})}{\tau_p + \beta_p + C_{p1}} + \frac{\beta_p(1 + C_{p2})^2}{(\tau_p + \beta_p + C_{p1})^2}\right] k_p[M]_p[Y_0]_p V_p + (\text{inflow} - \text{outflow})^{Q_2}_{j,L} \tag{A54}$$

Since there is no dead polymer in the monomer rich phase, the following relationship holds:

$$[Q_i]_p = [Q_i]\frac{V_s}{V_p} \tag{A55}$$

Now consider the postgel region where we can write expressions for the molecular weight of only the sol polymer. Since there is no gel in the monomer rich phase, the postgel radical moments are the same as those in pregel region. However they differ in the polymer rich phase.

$$[Y_0]_p = [R]_p \tag{A56}$$

$$[Y_0]_g = [R]_g \tag{A57}$$

$$[Y_1]_p = \frac{k_p[M]_p[Y_0]_p + k_{fm}[M]_p[Y_0]_T = k_{fts}[TS]_p[Y_0]_T + k_{fp}[Y_0]_T[Q_2]_p + k_\beta[Y_0]_T}{(k_{tcss} + k_{tdss})[Y_0]_p + (k_{tcsg} + k_{tdsg})[Y_0]_g + k_{fm}[M]_p + k_{fts}[TS]_p + k_{fp}[Q_1]_p + k_{fp}[M_g] + k_\beta} \tag{A58}$$

$$[Y_2]_p = \frac{k_{fm}[M]_p[Y_0]_T + k_{fts}[TS]_p[Y_0]_T + k_\beta[Y_0]_T + 2k_p[M]_p[Y_1]_p + k_{fp}[Q_3]_p[Y_0]_T}{k_{fm}[M]_{fp} + k_{fts}[TS]_p + k_\beta + k_{fp}[Q_1]_p + k_{fp}[M_g] + (k_{tcss} + k_{tdss})[Y_0]_p + (k_{tcsg} + k_{tdsg})[Y_0]_g} \tag{A59}$$

where

$$[Y_0]_T = [Y_0]_g + [Y_0]_p \tag{A60}$$

The polymer moments are given by:

$$V_s \frac{d[Q_0]}{dt} = (\text{inflow} - \text{outflow})^{Q_0}_{j,L} + k_{fm}[M]_m[Y_0]_m V_m + k_{fm}[M]_p[Y_0]_p V_p + \frac{1}{2} k_{tc}[Y_0]^2_m V_m + \frac{1}{2} k_{tcss}[Y_0]^2_p V_p + k_{td}[Y_0]^2_m V_m + k_{tdss}[Y_0]^2_p V_p + k_{tdsg}[Y_0]_p[Y_0]_g V_p - k_{fp}[Y_0]_g[Q_1]_p V_p + k_{fp}[Y_0]_p[M_g] V_p + k_\beta[Y_0]_m V_m + k_\beta[Y_0]_p V_p + k_{fts}[TS]_m[Y_0]_m V_m + k_{fts}[TS]_p[Y_0]_p V_p \tag{A61}$$

$$[Q_1] = [P_1] + [P_2] - [M_g] \tag{A62}$$

$$V_s \frac{d[Q_2]}{dt} = (\text{inflow} - \text{outflow})^{Q_2}_{i,L} + k_{fm}\{[M]_m[Y_2]_m V_m + [M]_p([Y_0]_g + [Y_0]_p) V_p\} + k_{fts}\{[TS]_m[Y_2]_m V_m + [TS]_p([Y_0]_g + [Y_0]_p) V_p\} + k_\beta\{[Y_2]_m V_m + ([Y_0]_g + [Y_0]_p) V_p\} + 2k_p[M]_p[Y_1]_p V_p + k_{tc}([Y_0]_m[Y_2]_m V_m + [Y_1]^2_m V_m) + k_{td}[Y_0]_m[Y_2]_m V_m + k_{tcss}[Y_1]^2_p V_p - k_{tcsg}[Y_0]_g[Y_2]_p V_p \tag{A63}$$

where the moles of monomer bound as gel is given by

$$V_s \frac{d[M_g]}{dt} = (\text{inflow} - \text{outflow})^{M_g}_{j,L} + k_p[M]_p[Y_0]_g V_p + k_{tcsg}[Y_0]_g[Y_1]_g V_p - k_\beta[Y_0]_g V_p \tag{A64}$$

In the postgel region the polymer moment equations are not closed. We have selected the closure method of Hulburt and Katz (1964) to express Q_3 as a function of the lower moments.

$$[Q_3] = \frac{[Q_2]}{[Q_1][Q_0]} (2[Q_2][Q_0] - [Q_1]^2) \tag{5}$$

The short chain branching frequency is given by

$$V_s \frac{d[SCB]}{dt} = (\text{inflow} - \text{outflow})^{SCB}_{j,L} + k_b[Y_0]_m V_m + k_b[Y_0]_p V_p + k_{pts}[Y_0]_m[TS]_m V_m + k_{pts}[Y_0]_p[TS]_p V_p \tag{A65}$$

We do not consider backbiting the gel radicals, or the consumption of short chain branched sol polymer by the gel. In the pregel region, the long chain branching frequency is given by:

$$V_s \frac{d[LCB]}{dt} = (\text{inflow} - \text{outflow})^{LCB}_{j,L} + k_{fp}[Y_0]_p[Q_1]_p V_p \tag{A66}$$

In the postgel region, considering branches only in the sol:

$$V_s \frac{d[LCB]}{dt} = (\text{inflow} - \text{outflow})^{LCB}_{j,L} + k_{fp}([Y_0]_p + [Y_0]_g)[Q_1]_p V_p \tag{A67}$$

This equation neglects the consumption of branches from the sol caused by incorporation of branched polymer into the gel. The number of short and long chain branches per 1,000 carbon atoms is given by (assuming two backbone carbon atoms per monomer unit):

$$\lambda_s = 500 \frac{[SCB]}{[Q_1]} \tag{A68}$$

$$\lambda_L = 500 \frac{[LCB]}{[Q_1]} \tag{A69}$$

Energy balance

The energy balance for any reaction volume, assuming no losses to the surroundings, is given by:

$$\frac{dH}{dt} = (m_1F_1 + m_2F_2)Cp_{\text{feed}}(T_{\text{feed}} - T_{\text{ref}}) + \rho_{\text{in}}Q_{\text{in}}Cp_{\text{in}}(T_{\text{in}} - T_{\text{ref}}) + \rho_{r,in}Q_{r,\text{in}}Cp_{r,\text{in}}(T_{r,\text{in}} - T_{\text{ref}}) - \rho(Q_{r,\text{out}} + Q_{\text{out}})Cp(T - T_{\text{ref}}) - \Delta H_{\text{rxn}}R_pV_s \quad \text{(cal/s)} \tag{A70}$$

where $\Delta H/(m_1Cp) = 1{,}300°\text{C}$.

Manuscript received Mar. 24, 1992, and revision received July 16, 1992.